Whole-Exome-Sequencing-Based Discovery of Human FADD Deficiency

Alexandre Bolze,[1] Minji Byun,[1,13] David McDonald,[2,13] Neil V. Morgan,[3,13] Avinash Abhyankar,[1,13] Lakshmanane Premkumar,[4,13] Anne Puel,[5] Chris M. Bacon,[6] Frédéric Rieux-Laucat,[7] Ki Pang,[8] Alison Britland,[9] Laurent Abel,[1,5] Andrew Cant,[2,10] Eamonn R. Maher,[3,11] Stefan J. Riedl,[4] Sophie Hambleton,[2,10] and Jean-Laurent Casanova[1,5,12,*]

Germline mutations in *FASL* and *FAS* impair Fas-dependent apoptosis and cause recessively or dominantly inherited autoimmune lymphoproliferative syndrome (ALPS). Patients with ALPS typically present with no other clinical phenotype. We investigated a large, consanguineous, multiplex kindred in which biological features of ALPS were found in the context of severe bacterial and viral disease, recurrent hepatopathy and encephalopathy, and cardiac malformations. By a combination of genome-wide linkage and whole-exome sequencing, we identified a homozygous missense mutation in *FADD*, encoding the Fas-associated death domain protein (FADD), in the patients. This *FADD* mutation decreases steady-state protein levels and impairs Fas-dependent apoptosis in vitro, accounting for biological ALPS phenotypes in vivo. It also impairs Fas-independent signaling pathways. The observed bacterial infections result partly from functional hyposplenism, and viral infections result from impaired interferon immunity. We describe here a complex clinical disorder, its genetic basis, and some of the key mechanisms underlying its pathogenesis. Our findings highlight the key role of FADD in Fas-dependent and Fas–independent signaling pathways in humans.

Germline mutations in *FASL*[1] (MIM 134638) and *FAS*[2,3] (MIM 134637) are genetic etiologies of autoimmune lymphoproliferative syndrome (ALPS [MIM 601859]) in humans. ALPS typically begins in early childhood (median age at onset: 2 yrs), with lymphadenopathy and/or splenomegaly. About half the patients have autoimmune disease, autoimmune cytopenias being particularly common.[4,5] The patients do not suffer from unusually severe infection, unless they are on immunosuppressive treatment,[4] and display no overt developmental phenotype. We investigated the molecular basis of a condition affecting at least four members of an extended consanguineous kindred of Pakistani origin (Figure 1A) with biological features of ALPS (high-circulating $CD4^{-}CD8^{-}TCR\alpha\beta^{+}$ T-cell [DNT] counts, and elevated IL-10 and FasL serum levels), no clinical features of ALPS, a complex infectious phenotype with both viral and bacterial infections, and congenital cardiovascular malformations (Table 1 and Table S1 available online). This study was approved by the local institutional review board. Written informed consent for participation in the study was obtained from all patients and family members studied.

The affected children suffered from recurrent, stereotypical episodes of fever, encephalopathy, and mild liver dysfunction (modestly elevated transaminases without cholestasis, metabolic derangement, or synthetic defects), sometimes accompanied by generalized seizures that were difficult to control. Episodes lasted several days, sometimes requiring intensive care, and cranial imaging in three patients (P1, P3, and P4 [IV.2, IV.4, and IV.5 in Figure 1]) suggested atrophy, despite subsequent recovery in two of these patients (P1 and P3). For some of the episodes, it was possible to identify a viral trigger: varicella zoster virus (VZV), measles mumps rubella (MMR) attenuated vaccine, parainfluenza virus, and Epstein-Barr virus (EBV). The index case, P3 (IV.4 in Figure 1), died at the age of 4 yrs, during such an episode. In addition, fatal invasive pneumococcal disease occurred in two children (P1 and P2 [IV.2 and IV.3 in Figure 1]), and Howell-Jolly bodies were detected in the two remaining patients (P3 and P4 [IV.4 and IV.5 in Figure 1]), despite the presence of a spleen (indicating functional hyposplenism).[6–8] This clinical syndrome has never before been described (no MIM number). In the previous generation, another five family

[1]St Giles Laboratory of Human Genetics of Infectious Diseases, Rockefeller Branch, The Rockefeller University, New York, NY 10065, USA; [2]Institute of Cellular Medicine, Newcastle University Medical School, Newcastle upon Tyne NE2 4HH, UK; [3]Wellchild Paediatric Research Centre and Centre for Rare Diseases and Personalised Medicine, School of Clinical and Experimental Medicine , University of Birmingham College of Medical and Dental Sciences, Edgbaston, Birmingham B152TT, UK; [4]Apoptosis and Cell Death Research Program, Sanford Burnham Medical Research Institute, La Jolla, CA 92037, USA; [5]Laboratory of Human Genetics of Infectious Diseases, Necker Branch, Institut National de la Santé et de la Recherche Médicale, U980, University Paris Descartes, Paris 75015, France; [6]Northern Institute for Cancer Research, Newcastle University and Department of Cellular Pathology, Newcastle upon Tyne Hospitals, Newcastle upon Tyne NE2 4HH, UK; [7]Normal and Pathologic Development of the Immune System Research Laboratory, U768, Institut National de la Santé et de la Recherche Médicale (INSERM); Unit of Pediatric Immunology and Hematology, Necker Hospital (APHP); University Paris Descartes, Paris 75015, France; [8]Paediatric Neurology Dept, Great North Children's Hospital, Newcastle upon Tyne NE1 4LP, UK; [9]Children's Unit, Airedale General Hospital, West Yorkshire BD20 6TD, UK; [10]Paediatric Immunology Dept, Great North Children's Hospital, Newcastle upon Tyne NE1 4LP, UK; [11]West Midlands Region Genetics Service, Birmingham Women's Hospital, Edgbaston, Birmingham B152TG, UK; [12]Pediatric Immunology-Hematology Unit, Necker Hospital for Sick Children, Paris 75015, France
[13]These authors contributed equally to this work
*Correspondence: jean-laurent.casanova@rockefeller.edu
DOI 10.1016/j.ajhg.2010.10.028.

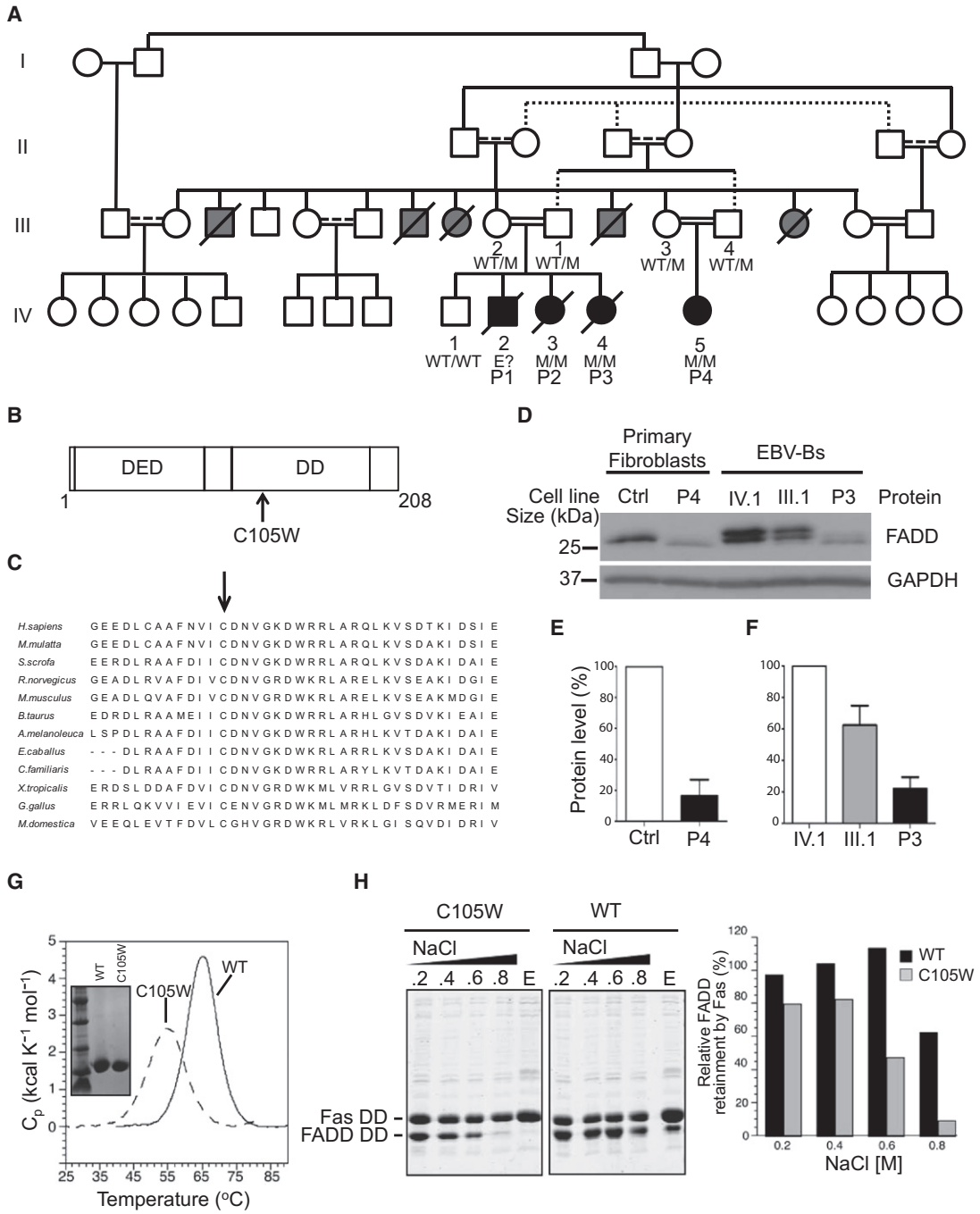

Figure 1. Characterization of an Inherited *FADD* Mutation

(A) Pedigree of the Pakistani family. Black symbols indicate patients. Gray symbols indicate siblings in the parents' generation who died early in childhood with clinical symptoms related to the disorder observed in P1–P4. Clinical information was incomplete for these members of the parents' generation. Haplotypes of *FADD* are indicated: M stands for c.315T>G, and WT for the wild-type allele.

(B) Schematic diagram of FADD protein showing the death effector domain (DED) and the death domain (DD). The location corresponding to the mutation is indicated by an arrow, and the predicted amino acid substitution is shown.

(C) Evolutionary conservation of the FADD region containing amino acid residue C105 (indicated by the arrow).

(D) FADD immunoblot in primary fibroblasts and EBV-B cells from patients and controls. Experiments were carried out with two different antibodies: a mouse monoclonal antibody against the C terminus of FADD (#610399, BD Biosciences) and a rabbit polyclonal antibody against the residues surrounding Ser194 in human FADD (#2782, Cell Signaling). Similar results were obtained with both antibodies. GAPDH was used as a loading control. A representative blot with the monoclonal antibody is shown (n = 6).

(E and F) FADD protein levels in primary fibroblasts (E) and EBV-B cells (F) determined on the basis of the intensity of the signal on immunoblots and normalized with respect to GAPDH levels. A mean of six experiments is shown. Error bars indicate the SEM.

(G and H) Effect of the C105W mutation on the stability of FADD DD folding and the Fas-FADD complex. (G) Differential scanning calorimetry (DSC) analysis of WT and C105W His_6-FADD DD proteins. (H) Fas-FADD complex stability assay. The retention of FADD DD (WT or C105W) with immobilized His_6-Fas DD was assessed with various concentrations of NaCl, as previously described[19] (E: imidazole elution of remaining complex after the final NaCl concentration).

Table 1. Clinical Features of Four Patients in the Family

Patient		P1	P2	P3	P4
Gender		male	female	female	female
Cardiovascular malformation		none	none	yes (pulmonary atresia) + ventricular septal defect	yes (L-sided SVC draining to left atrium)
Functional hyposplenism	**spleen size**	NA	normal	normal	normal
	Howell-Jolly bodies	NA	NA	yes	yes
	invasive pneumococcal infection	yes (meningitis, 4 mo)	yes (septicemia, 14 mo)	no[a]	no[a]
Features of febrile episodes	**documented viral trigger**	VZV		VZV, HHV6	MMR vaccine, astrovirus, parainfluenza virus 2, EBV
	encephalopathy	yes	yes	yes	yes
	seizures	yes	yes	yes	yes
	liver dysfunction (maximal ALT, IU/L)	yes (NA)	yes (NA)	yes (1042)	yes (383)
ALPS phenotype	**autoimmune disease**	no	no	no	no
	presence of autoantibodies	NA	NA	no[b]	yes[b] (antierythrocyte antibodies intermittently present)
	lymphadenopathy or splenomegaly	no	no	no	no
	percentage of $CD4^-CD8^-TCR\alpha\beta^+$ T cells	NA	NA	NA	7.8
	lymphocyte apoptosis	NA	NA	NA	impaired
	serum FasL	NA	NA	NA	high
	serum IL-10	NA	NA	NA	high
CNS outcome	**neurodevelopmental progress**	NA	within normal limits	within normal limits	within normal limits
	cerebral atrophy on CT/MRI (age)	yes (4 mo)	NA	yes (3 mo)	mild (5 mo) + increased at 2.5 yr + spotty calcification of subcortical white matter
Liver histology		NA	mild chronic portal inflammation with bridging fibrosis	NA	mild chronic portal inflammation with mild fibrosis
Follow-up data		died at 4 mo	died at 14 mo	died at 4 yr and 4 mo.	alive and currently 2 yr and 9 mo.

Abbreviations are as follows: ALT, alanine transaminase; FasL, Fas ligand; HHV6, Human Herpesvirus Six; IL-10, interleukin 10; NA, not assessed.
[a] On antibacterial prophylaxis from early infancy.
[b] Autoantibody screen including antinuclear, anti-smooth muscle, antimitochondrial, and anti-gastric parietal cell antibodies, direct antiglobulin test.

members had died in childhood, two with "epilepsy" and two from infection (pneumonia and measles, respectively) (data not shown), suggesting that there may have been up to nine patients with this disorder in these two generations of this kindred.

We hypothesized that this syndrome would segregate as an autosomal-recessive trait. We investigated its genetic etiology, by combining genome-wide linkage analysis by homozygosity mapping with whole-exome sequencing.[9–11] For the linkage analysis, we genotyped three affected patients (P2, P3, and P4), their parents (III.1, III.2, III.3, and III.4), and one healthy sibling (IV.1) with the Affymetrix 500K SNP Array or the Affymetrix 6.0 Array. No material was available for P1. Homozygous regions

were detected with the HomozygosityMapper genome browser. Two regions (> 1 Mb) were homozygous in the three affected patients and heterozygous in other members of the family: an 8 Mb region on chromosome 11 (between rs4930243 and rs7926553; bp position: g.68,499,874–g.76,470,079; hg18, NCBI 36.1) and a 9 Mb region on chromosome 18 (between rs9959449 and rs12327522; bp position: g.60,703,632–g.70,387,399; hg18, NCBI 36.1). The regions were further confirmed by typing microsatellite markers (Figure S1).

In parallel to the linkage analysis, we sequenced the exome of P3 with the SureSelect Human All Exon Kit (Agilent Technologies). The sequences obtained were aligned to the reference genome (hg18 build) with the Burrows-Wheeler Aligner. Three open-source packages were used for downstream processing and variant calling: the Genome Analysis Toolkit (GATK),[12] SAMtools,[13] and Picard Tools. Substitution calls were made with the GATK UnifiedGenotyper. All calls with a read coverage < 4× and a phred-scaled SNP quality of < 30 were filtered out. All the variants were annotated with SeattleSeq SNP Annotation. In total, we identified 23,146 variations. Of these, 67 variants were found in the chromosome 11 candidate region, and 14 variants were found in the chromosome 18 candidate region (Table S2). Comparisons with the NCBI dbSNP build 129, the 1000 Genomes Project database, and our in-house database (composed of 70 exomes) identified only one nonsynonymous variant that had not been reported before and mapped to the chromosome 11 region. No previously unreported nonsynonymous variant mapping to the linked region on chromosome 18 was identified. The variant identified was a missense homozygous c.315T>G in exon 2 of *FADD* (NM_003824.3, MIM 602457) that changes cysteine at amino acid position 105 to tryptophan, p.C105W (referred to as C105W hereafter) (Figure 1B and Figure S2). Cysteine at amino acid position 105 is highly conserved throughout evolution (Figure 1C). We validated this variant by Sanger sequencing on genomic DNA from peripheral blood and on cDNA from EBV-transformed B cells (EBV-B). This variant segregated with the disease status in all family members examined (Figure 1A) and was not found in 282 Pakistani controls, suggesting that it is not an irrelevant polymorphism.

FADD was first described as an adaptor protein interacting with the apoptosis-inducing surface receptor Fas.[14] It has since been shown to interact with various partners and to participate in many other cellular processes, such as autophagy, inflammation, innate immunity, cell proliferation, and tumor development.[15–18] Thus, we hypothesized that the FADD mutation was responsible for the complex clinical phenotype of the affected individuals. To test this hypothesis, we assessed the expression of *FADD* mRNA levels in EBV-B cells by quantitative RT-PCR. We found that *FADD* mRNA levels in the EBV-B cells from P3 (C105W/C105W) were similar to those in the EBV-B cells from IV.1 (WT/WT) (data not shown). However, FADD protein levels were clearly lower in primary fibroblasts from P4 (~16%) than in primary fibroblasts from a healthy control (Figures 1D and 1E). Similarly, FADD protein levels were lower in the EBV-B cells from P3 (~21%) and III.1 (WT/C105W) (~62%) than in the EBV-B cells from IV.1 (Figures 1D and 1F). Residue C105 is located in alpha-helix 1 of the FADD death domain (DD), at the interface of the Fas-FADD complex.[19] We tested the effect of the C105W mutation on FADD folding stability and Fas-FADD interaction with recombinant Fas DD and FADD DD proteins. The C105W mutant protein was folded, as shown by differential scanning calorimetry (DSC), but the folding stability of the mutant protein was lower than that of WT FADD, by ~10°C (Figure 1G). We then assessed the effect of the mutation on Fas-FADD complex stability by using a gel copurification assay in the presence of increasing concentrations of NaCl (Figure 1H). Binding levels for C105W FADD and Fas were clearly lower than those for WT FADD, suggesting that the primary Fas-FADD complex was less stable. Thus, the C105W mutation in FADD strongly decreases steady-state protein levels and impairs the interaction of the residual FADD protein with Fas.

FADD forms a critical bridge between the death receptor Fas and caspase-8 (MIM 601763), in a multimolecular array known as the death-inducing signaling complex (DISC).[20,21] We therefore studied Fas-induced apoptosis in the patients' cells. Phytohemagglutinin-stimulated peripheral-blood lymphocytes (PHA blasts) from P4 displayed impaired apoptosis (viability >50% higher than for controls) when challenged with cross-linked Fas ligand (FasL), similar to Fas-deficient cells (Figure 2A). In addition, EBV-B cells from P3 displayed impaired apoptosis when Fas was crosslinked with agonistic Fas-specific antibody (Apo1.3) (Figure 2B). In keeping with this finding, investigations of the surviving patient P4 revealed several features classically associated with ALPS due to Fas[2,3] or FasL[1] deficiency and more rarely associated with deficiencies of caspase-8 or caspase-10 (MIM 601762).[4,22,23] P4 displayed an expansion of the population of mature $CD4^{-}CD8^{-}TCR\alpha\beta^{+}$ T cells (DNT) in peripheral blood, as well as elevated serum levels of IL-10 and soluble FasL (Table 1 and Figures 2C and 2D).[24,25] Our data confirm that the FADD C105W variant impairs apoptotic function both in vitro and in vivo, resulting in biological features of ALPS despite the lack of clinically evident autoimmunity or lymphoproliferation (although P4 did have transiently detectable antierythrocyte autoantibodies and P2, P3, and P4 displayed peripheral lymphocytosis [Table S1]). T cell proliferation in response to various stimuli was normal (Figure 2E), in contrast with findings for caspase-8 deficient individuals[22] and mice with FADD deficiency specific to T or B cells.[26] A recent study in mice suggested that FADD deficiency may decrease T cell proliferation as a result of an excess of necroptosis.[16] To examine whether C105W affected necroptosis, we added an inhibitor of necroptosis, necrostatin 1, to CD3- and CD28-stimulated proliferation assays.

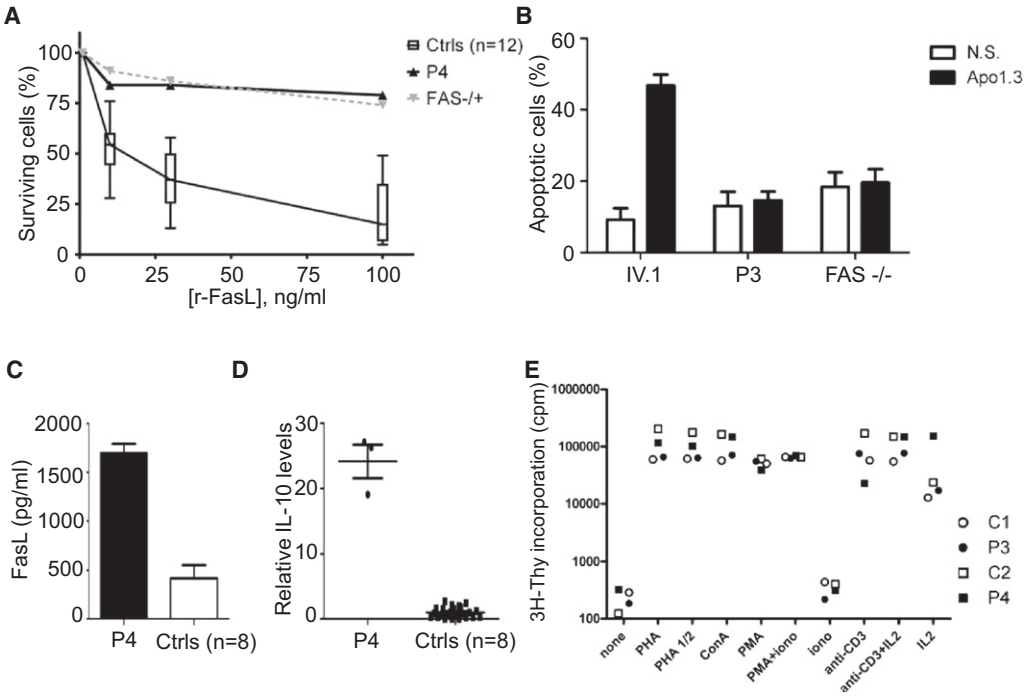

Figure 2. Characterization of the ALPS Phenotype

(A) PHA blasts from normal volunteers (Ctrls), patient P4, and a heterozygous Fas-deficient patient were stimulated with recombinant FasL (r-FasL), and cell viability was analyzed. The proportion of live cells in the presence of r-FasL is displayed as a percentage of live cells in the presence of enhancer alone, for each sample. Error bars indicate the SEM.

(B) EBV-B cells from P3, IV.1, and a Fas-deficient patient were treated with an antibody against Fas (Apo-1.3), in the presence of rabbit anti-mouse Ig (Ramig), for 6 hr and analyzed for early apoptosis. The percentage of cells that were apoptotic was calculated as the percentage of cells positive for AnnexinV and negative for propidium iodide staining. NS indicates that the cells were incubated with Ramig only. A mean of three independent experiments is shown. Error bars indicate the SEM.

(C) FasL levels in the serum of P4 and eight healthy controls (Ctrls). Error bars indicate the SEM.

(D) IL-10 levels in the serum of P4 and eight healthy controls. IL-10 values were normalized with respect to the mean of the control samples. Error bars indicate the SEM.

(E) Proliferation assay. Proliferative responses to various stimuli (PHA, 5 μg/ml; IL-2, 500 U/ml; concanavalin A, 5 μg/ml; anti-CD3 [OKT3], 0.1 μg/ml; PMA, 50 ng/ml; ionomycin, 0.1 μg/ml). P3 and P4 responded similarly in comparison to the two controls, C1 and C2.

Necrostatin-1 did not affect proliferative responses in this system (Figure S3).

The laboratory findings for the FADD-deficient patients were typical of ALPS, but clinical presentation was dominated by features absent from classical ALPS, leading to early death. These features included invasive pneumococcal disease (IPD), which killed both P1 and P2. Neither P3 nor P4 suffered from IPD, probably because they were on antibacterial prophylaxis from early infancy, but abnormally high counts of Howell-Jolly bodies were seen on their blood smears. The identification of Howell-Jolly bodies on peripheral-blood smears is the most reliable indicator of impaired splenic phagocyte function (including functional or anatomical asplenia).[6–8] Moreover, asplenia (MIM 271400 and MIM 208530)—whether anatomical or functional, congenital or acquired—has frequently been associated with a strong predisposition to infections by encapsulated bacteria, such as IPD, in particular.[6–8,27] For example, we showed that 15 of 20 patients with isolated congenital asplenia (ICA) suffered from invasive bacterial infections, caused mostly by *Streptococcus pneumoniae* (61%).[27] Finally, B cell responses to vaccine antigens appeared to be intact in the patients (Table S1), ruling out other known causes of IPD.[28] These observations suggest that functional hyposplenism underlies IPD in FADD-deficient patients.

In addition to IPD, FADD-deficient patients suffered from recurrent episodes of encephalopathy and liver dysfunction with fever, which were sometimes triggered by viral infection (Table 1). Previous studies in mouse embryonic fibroblasts (MEFs) suggested that FADD plays a crucial role in type I interferon (IFN) -dependent antiviral immunity.[15,29] We therefore tested the hypothesis that the unusually severe illnesses associated with viral infections in FADD-deficient patients might be due to an impaired type I IFN-dependent antiviral response, by assessing the antiviral effect of IFN-α in vesicular stomatitis virus (VSV)-infected P3 and IV.1 EBV-B cells. STAT1-deficient EBV-B cells, lacking a key type-I-IFN-responsive pathway,[29–31] were included as controls. Prior treatment with IFN-α protected both P3 and IV.1 cells from VSV-induced cell death until 36 hr after infection (Figure 3A). However, IFN-α-treated P3 cells eventually succumbed to VSV infection, whereas IFN-α-treated IV.1 cells remained protected

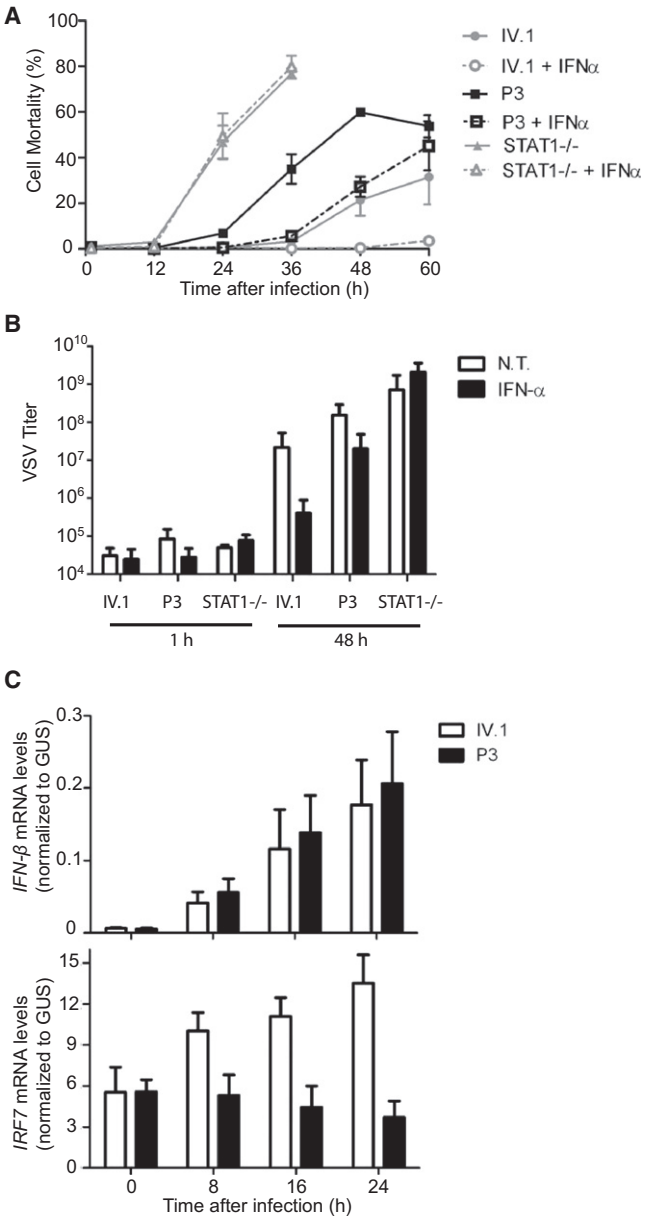

Figure 3. Impaired Antiviral Immunity

(A) EBV-B cells from P3, IV.1, and a STAT1-deficient patient were infected with VSV at a multiplicity of infection (MOI) of 1, with or without prior treatment with 100 IU/ml of IFN-α for 24 hr. Cell mortality was assessed by measuring the amount of LDH released into the medium. For STAT1-deficient cells, results are shown only until 36 hr after infection because of high levels of spontaneous LDH release at later time points. A mean of three independent experiments is shown. Error bars indicate the SEM.

(B) EBV-B cells from P3, IV.1, and a STAT1-deficient patient were either left untreated (NT, bars in white) or treated with 100 IU/ml IFN-α for 24 hr (IFN-α, bars in black), prior to infection with VSV at a MOI of 0.1, and were harvested 48 hr after infection. VSV titers (TCID50, ml) were determined on Vero cells. A mean of three independent experiments is shown. Error bars indicate the SEM.

(C) EBV-B cells from P3 or IV.1 were infected with VSV at a MOI of 10. Cells were harvested at the indicated time points, and total RNA was extracted. *IFN-β* and *IRF7* mRNA levels were determined by quantitative RT-PCR. Threshold cycles normalized with respect to those of GUS (ΔC_T) are plotted as $2^{-\Delta CT}$. A mean of three independent experiments is shown. Error bars indicate the SEM.

until 60 hr after infection (Figures 3A and 3B). These results suggest that the IFN-α-responsive pathway is intact but that the positive feedback of IFN signaling is impaired in FADD-deficient cells. Interferon regulatory factor 7 (IRF7), induced by autocrine type I IFNs, is known to play a critical role in the positive feedback of IFN signaling, by inducing IFN-α gene family members. We found that the induction of IRF7 in response to VSV infection was impaired in P3 cells, despite levels of IFN-β induction similar to those in IV.1 cells (Figure 3C). These data provide a molecular basis for the increase in susceptibility to viral diseases in FADD-deficient patients.

By contrast, we can only speculate about the mechanisms underlying the developmental abnormalities within this kindred. P3 displayed pulmonary atresia (MIM 178370) and P4 had a left-sided superior vena cava (SVC) draining into the left atrium, both of which are rare as sporadic defects and were probably caused by FADD insufficiency. Indeed, mice with a null mutation in *FADD* are not viable because of embryonic defects, including cardiac abnormalities, such as thinning of the ventricular myocardium.[32] Moreover, *FADD* expression in mice, at embryonic day 11.5, is detected not only in the myocardium but also in the brain, liver, and developing vertebrae.[32] Spinal anatomy appeared normal in all FADD-deficient patients, but hepatic and cerebral dysfunctions were clearly key elements of the disease phenotype. Cerebral atrophy was observed in P1, P3, and P4 at a very early age and appeared to be progressive in P4 (scan images in Figure S4), despite continuing neurodevelopment (Table 1). This, and the mild portal fibrosis observed on liver biopsy in two patients (Figures 4J–4L), should be considered as sequelae of FADD deficiency. Finally, FADD seems to be important for the development of a functional spleen in humans, as demonstrated by the presence of Howell-Jolly bodies—the hallmark of a lack of splenic function—in the blood smears of P3 and P4.[7,8] In P2, a limited postmortem examination of lymph nodes, spleen, and thymus revealed no histological features of ALPS or other lymphoid tissue abnormalities (Figure 4). However, the spleen showed an expanded, congested red pulp containing increased neutrophils, consistent with sepsis. Moreover, the normal cord-sinus architecture of the red pulp was not readily apparent; reticulin deposition appeared disordered, normal sinusoidal "barrel hoop" fibers were not identified, and macrophages appeared haphazardly arranged (Figures 4C–4I). Examination of spleen histology in other affected individuals is unlikely to be possible, thus precluding firm conclusions regarding the relationship between human FADD deficiency and disordered red pulp microarchitecture. The prominence but incomplete penetrance of cardiac, cerebral, hepatic, and splenic abnormalities in the clinical phenotype strongly suggests the existence of organ-specific effects of FADD deficiency worthy of further study in suitably designed mouse models.

In conclusion, we have described the clinical features of an autosomal-recessive inherited disorder with biological

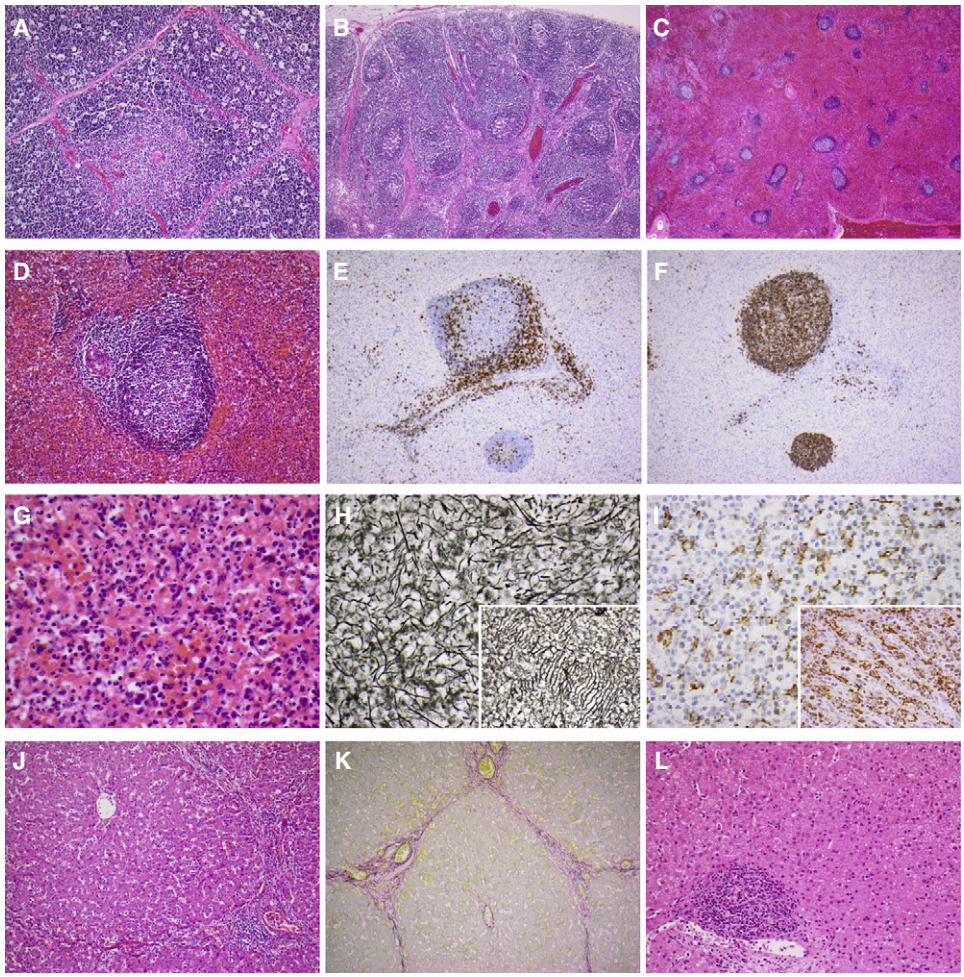

Figure 4. Histopathology of P2 and P4
(A–K) postmortem histopathology of P2 at 14 months.
(A) Normal thymic architecture; increased cortical tingible body macrophages consistent with a stress response (P2, hematoxylin and eosin [H&E] stain, original magnification × 100).
(B) Normal-appearing reactive lymph node with follicular hyperplasia (P2, H&E stain, original magnification × 40).
(C) Low-power view of the spleen showing expanded, congested red pulp with relatively reduced white pulp (P2, H&E stain, original magnification × 20).
(D) White pulp nodule containing a follicle with a reactive germinal centre, but no marginal zone hyperplasia, arising from a periarteriolar lymphoid sheath (P2, H&E stain, original magnification × 200).
(E) Immunohistochemistry for CD3 shows a normal distribution of CD3-positive T cells in a white pulp nodule (P2, Ventana Benchmark XT immunostainer, monoclonal antibody LN10, original magnification × 100).
(F) Immunohistochemistry for CD20 shows a normal distribution of CD20-positive B cells in a white pulp nodule (P2, Ventana Benchmark XT immunostainer, monoclonal antibody L26, original magnification × 100).
(G) Congested, disorganized red pulp containing increased neutrophils consistent with sepsis (P2, H&E stain, original magnification × 400).
(H) Disorganized reticulin staining pattern of splenic red pulp. Inset: "barrel hoop" arrangement of sinusoidal reticulin fibers in a normal control spleen (P2, Gordon and Sweet's reticulin stain, original magnification × 400).
(I) Immunohistochemistry for CD68 shows a haphazard arrangement of macrophages in the splenic red pulp. Inset: orderly distribution of cordal macrophages in a normal control spleen (P2, Ventana Benchmark XT immunostainer, monoclonal antibody PG-M1, original magnification × 400).
(J) Liver showing portal-portal linkage and expansion of portal tracts by a moderate chronic inflammatory cell infiltrate without interface activity (P2, H&E stain, original magnification × 100).
(K) Sirius red staining of liver shows collagen deposition (red) within portal-portal bridges. Elastin could also be demonstrated (not shown), consistent with established portal-portal fibrosis (P2, Sirius red and Fast green stain, original magnification × 100).
(L) Histopathology of P4 at 22 months. The liver shows mild expansion of portal tracts by a chronic inflammatory cell infiltrate but no bridging fibrosis (H&E stain, original magnification × 200).

features of ALPS, susceptibility to bacterial and viral infections, and developmental abnormalities. Furthermore, we have determined its genetic etiology, which results in FADD deficiency in the affected children, by genome-wide linkage analysis and whole-exome sequencing. Finally, we have dissected the molecular mechanisms of

disease for several aspects of this phenotype, including bacterial susceptibility (functional hyposplenism), viral susceptibility (impaired IFN immunity), and features of ALPS (impaired Fas-dependent apoptosis). Other phenotypes, particularly those of a developmental nature, remain unexplained but are probably due to the disruption of Fas-independent pathways, given that they were not documented in Fas-deficient patients. These unanticipated findings highlight the power of exome sequencing used in combination with genome-wide linkage analysis within consanguineous families.[9–11,33] We anticipate rapid advances in molecular medicine,[5,9] facilitated by this strategy, in the coming years.

Supplemental Data

Supplemental Data include four figures and two tables and can be found with this article online at http://www.cell.com/AJHG/.

Acknowledgments

We thank the patients' family for their trust and all members of our laboratories for helpful discussions. We thank Capucine Picard for her expert analysis of the lymphocyte subsets of the patients. We thank Louise Tee for technical assistance and SNP genotyping and Shanaz Pasha for patient ascertainment. We thank Magorzata Dobaczewska for the production of proteins in bacteria and Andrey Bobkov (protein facility at SBMRI) for DSC measurement. The Laboratory of Human Genetics of Infectious Diseases is supported by grants from INSERM, University Paris Descartes, The Rockefeller University Center for Clinical Translational Science (grant number 5UL1RR024143-03), The Rockefeller University, and St. Giles Foundation. The laboratory of S.H. is supported by an MRC grant (G0701897). This work was also supported by a R01AA017238 grant to S.J.R., by an ANR grant (ANR-08-GENO-015-01) to F.R.L., and by the WellChild foundation. M.B. is supported by a fellowship from the Cancer Research Institute.

Received: September 15, 2010
Revised: October 23, 2010
Accepted: October 27, 2010
Published online: November 24, 2010

Web Resources

The URLs for the data presented here are as follows:

1000 Genomes Project, http://www.1000genomes.org
HomozygosityMapper, http://www.homozygositymapper.org/
Online Mendelian Inheritance in Man (OMIM), http://www.ncbi.nlm.nih.gov/Omim/
Picard Tools, http://picard.sourceforge.net/
SeattleSeq SNP Annotation, http://gvs.gs.washington.edu/SeattleSeqAnnotation/

References

1. Del-Rey, M., Ruiz-Contreras, J., Bosque, A., Calleja, S., Gomez-Rial, J., Roldan, E., Morales, P., Serrano, A., Anel, A., Paz-Artal, E., and Allende, L.M. (2006). A homozygous Fas ligand gene mutation in a patient causes a new type of autoimmune lymphoproliferative syndrome. Blood *108*, 1306–1312.
2. Fisher, G.H., Rosenberg, F.J., Straus, S.E., Dale, J.K., Middleton, L.A., Lin, A.Y., Strober, W., Lenardo, M.J., and Puck, J.M. (1995). Dominant interfering Fas gene mutations impair apoptosis in a human autoimmune lymphoproliferative syndrome. Cell *81*, 935–946.
3. Rieux-Laucat, F., Le Deist, F., Hivroz, C., Roberts, I.A., Debatin, K.M., Fischer, A., and de Villartay, J.P. (1995). Mutations in Fas associated with human lymphoproliferative syndrome and autoimmunity. Science *268*, 1347–1349.
4. Su, H.C., and Lenardo, M.J. (2008). Genetic defects of apoptosis and primary immunodeficiency. Immunol. Allergy Clin. North Am. *28*, 329–351, ix.
5. Casanova, J.L., and Abel, L. (2007). Primary immunodeficiencies: a field in its infancy. Science *317*, 617–619.
6. Brigden, M.L. (2001). Detection, education and management of the asplenic or hyposplenic patient. Am. Fam. Physician *63*, 499–506, 508.
7. Doll, D.C., List, A.F., and Yarbro, J.W. (1987). Functional hyposplenism. South. Med. J. *80*, 999–1006.
8. Katcher, A.L. (1980). Familial asplenia, other malformations, and sudden death. Pediatrics *65*, 633–635.
9. Byun, M., Abhyankar, A., Lelarge, V., Plancoulaine, S., Palanduz, A., Telhan, L., Boisson, B., Picard, C., Dewell, S., Zhao, C., et al. (2010). Whole-exome sequencing-based discovery of STIM1 deficiency in a child with fatal classic Kaposi sarcoma. J. Exp. Med. *207*, 2307–2312.
10. Ng, S.B., Buckingham, K.J., Lee, C., Bigham, A.W., Tabor, H.K., Dent, K.M., Huff, C.D., Shannon, P.T., Jabs, E.W., Nickerson, D.A., et al. (2010). Exome sequencing identifies the cause of a mendelian disorder. Nat. Genet. *42*, 30–35.
11. Ng, S.B., Turner, E.H., Robertson, P.D., Flygare, S.D., Bigham, A.W., Lee, C., Shaffer, T., Wong, M., Bhattacharjee, A., Eichler, E.E., et al. (2009). Targeted capture and massively parallel sequencing of 12 human exomes. Nature *461*, 272–276.
12. McKenna, A., Hanna, M., Banks, E., Sivachenko, A., Cibulskis, K., Kernytsky, A., Garimella, K., Altshuler, D., Gabriel, S., Daly, M., and DePristo, M.A. (2010). The Genome Analysis Toolkit: a MapReduce framework for analyzing next-generation DNA sequencing data. Genome Res. *20*, 1297–1303.
13. Li, H., Handsaker, B., Wysoker, A., Fennell, T., Ruan, J., Homer, N., Marth, G., Abecasis, G., and Durbin, R.; 1000 Genome Project Data Processing Subgroup. (2009). The Sequence Alignment/Map format and SAMtools. Bioinformatics *25*, 2078–2079.
14. Chinnaiyan, A.M., O'Rourke, K., Tewari, M., and Dixit, V.M. (1995). FADD, a novel death domain-containing protein, interacts with the death domain of Fas and initiates apoptosis. Cell *81*, 505–512.
15. Balachandran, S., Thomas, E., and Barber, G.N. (2004). A FADD-dependent innate immune mechanism in mammalian cells. Nature *432*, 401–405.
16. Osborn, S.L., Diehl, G., Han, S.J., Xue, L., Kurd, N., Hsieh, K., Cado, D., Robey, E.A., and Winoto, A. (2010). Fas-associated death domain (FADD) is a negative regulator of T-cell receptor-mediated necroptosis. Proc. Natl. Acad. Sci. USA *107*, 13034–13039.
17. Walsh, C.M., and Bell, B.D. (2010). T cell intrinsic roles of autophagy in promoting adaptive immunity. Curr. Opin. Immunol. *22*, 321–325.
18. Tourneur, L., and Chiocchia, G. (2010). FADD: a regulator of life and death. Trends Immunol. *31*, 260–269.

19. Scott, F.L., Stec, B., Pop, C., Dobaczewska, M.K., Lee, J.J., Monosov, E., Robinson, H., Salvesen, G.S., Schwarzenbacher, R., and Riedl, S.J. (2009). The Fas-FADD death domain complex structure unravels signalling by receptor clustering. Nature *457*, 1019–1022.
20. Peter, M.E., and Krammer, P.H. (2003). The CD95(APO-1/Fas) DISC and beyond. Cell Death Differ. *10*, 26–35.
21. Taylor, R.C., Cullen, S.P., and Martin, S.J. (2008). Apoptosis: controlled demolition at the cellular level. Nat. Rev. Mol. Cell Biol. *9*, 231–241.
22. Chun, H.J., Zheng, L., Ahmad, M., Wang, J., Speirs, C.K., Siegel, R.M., Dale, J.K., Puck, J., Davis, J., Hall, C.G., et al. (2002). Pleiotropic defects in lymphocyte activation caused by caspase-8 mutations lead to human immunodeficiency. Nature *419*, 395–399.
23. Wang, J., Zheng, L., Lobito, A., Chan, F.K., Dale, J., Sneller, M., Yao, X., Puck, J.M., Straus, S.E., and Lenardo, M.J. (1999). Inherited human Caspase 10 mutations underlie defective lymphocyte and dendritic cell apoptosis in autoimmune lymphoproliferative syndrome type II. Cell *98*, 47–58.
24. Bleesing, J.J., Brown, M.R., Straus, S.E., Dale, J.K., Siegel, R.M., Johnson, M., Lenardo, M.J., Puck, J.M., and Fleisher, T.A. (2001). Immunophenotypic profiles in families with autoimmune lymphoproliferative syndrome. Blood *98*, 2466–2473.
25. Magerus-Chatinet, A., Stolzenberg, M.C., Loffredo, M.S., Neven, B., Schaffner, C., Ducrot, N., Arkwright, P.D., Bader-Meunier, B., Barbot, J., Blanche, S., et al. (2009). FAS-L, IL-10, and double-negative CD4- CD8- TCR alpha/beta+ T cells are reliable markers of autoimmune lymphoproliferative syndrome (ALPS) associated with FAS loss of function. Blood *113*, 3027–3030.
26. Wilson, N.S., Dixit, V., and Ashkenazi, A. (2009). Death receptor signal transducers: nodes of coordination in immune signaling networks. Nat. Immunol. *10*, 348–355.
27. Mahlaoui, N., Minard-Colin, V., Picard, C., Bolze, A., Ku, C.L., Tournilhac, O., Gilbert-Dussardier, B., Pautard, B., Durand, P., Devictor, D., et al. (2010). Isolated congenital asplenia: A French nationwide retrospective survey of 20 cases. J Pediatr.
28. Picard, C., Puel, A., Bustamante, J., Ku, C.L., and Casanova, J.L. (2003). Primary immunodeficiencies associated with pneumococcal disease. Curr. Opin. Allergy Clin. Immunol. *3*, 451–459.
29. Balachandran, S., Venkataraman, T., Fisher, P.B., and Barber, G.N. (2007). Fas-associated death domain-containing protein-mediated antiviral innate immune signaling involves the regulation of Irf7. J. Immunol. *178*, 2429–2439.
30. Chapgier, A., Wynn, R.F., Jouanguy, E., Filipe-Santos, O., Zhang, S., Feinberg, J., Hawkins, K., Casanova, J.L., and Arkwright, P.D. (2006). Human complete Stat-1 deficiency is associated with defective type I and II IFN responses in vitro but immunity to some low virulence viruses in vivo. J. Immunol. *176*, 5078–5083.
31. Chapgier, A., Kong, X.F., Boisson-Dupuis, S., Jouanguy, E., Averbuch, D., Feinberg, J., Zhang, S.Y., Bustamante, J., Vogt, G., Lejeune, J., et al. (2009). A partial form of recessive STAT1 deficiency in humans. J. Clin. Invest. *119*, 1502–1514.
32. Yeh, W.C., Pompa, J.L., McCurrach, M.E., Shu, H.B., Elia, A.J., Shahinian, A., Ng, M., Wakeham, A., Khoo, W., Mitchell, K., et al. (1998). FADD: essential for embryo development and signaling from some, but not all, inducers of apoptosis. Science *279*, 1954–1958.
33. Walsh, T., Shahin, H., Elkan-Miller, T., Lee, M.K., Thornton, A.M., Roeb, W., Abu Rayyan, A., Loulus, S., Avraham, K.B., King, M.C., and Kanaan, M. (2010). Whole exome sequencing and homozygosity mapping identify mutation in the cell polarity protein GPSM2 as the cause of nonsyndromic hearing loss DFNB82. Am. J. Hum. Genet. *87*, 90–94.